Generation and Characterization of Photopolymerized Polymer Brush Gradients

Bradley P. Harris[†] and Andrew T. Metters*[,†,‡]

Department of Chemical and Biomolecular Engineering and Department of Bioengineering, Clemson University, Clemson, South Carolina 29634

Received June 8, 2005; Revised Manuscript Received January 27, 2006

ABSTRACT: A novel method for using photoiniferter-mediated photopolymerization techniques to create surface-bound macromolecular assemblies exhibiting position-dependent molecular weights, surface densities, and layer thicknesses has been developed. By using a variable photomasking system and judiciously selecting photopolymerization parameters, such as monomer concentration and light intensity, poly(methyl methacrylate) (PMMA) surfaces exhibiting layer thickness gradients were photopolymerized on single silicon substrates from self-assembled monolayers of photoiniferter. The ability to precisely control the topographic slope of a surface-tethered polymer brush gradient was achieved by varying surface irradiation time or bulk monomer concentration. Kinetics of surface-gradient formation were measured using variable angle ellipsometry as well as transmission Fourier transform infrared spectroscopy. Under the conditions studied, the photopolymerization of PMMA exhibited first-order dependence of polymer brush layer thickness on both monomer concentration and surface irradiation time even though the polymer chain ends could not be reinitiated as should occur with a living-radical system.

Introduction

Traditional surface modification is performed by a variety of methods, including chemical reaction in solution, physical adsorption, and various irradiation techniques with subsequent graft polymerization.[1] However, these existing methods typically proceed in an all-or-nothing fashion and are not sufficient to produce dense arrays of well-defined polymer architectures with nanometer scale precision. The ability to control surface properties on the nanometer scale is especially important to the engineering of biomaterial surfaces where the surface is designed to elicit a desired cellular response.[2]

The fabrication of new polymeric materials exhibiting precise molecular weights, chain densities, and nanoarchitectures can be readily accomplished in bulk solution or from surfaces using controlled, chain growth polymerizations that proceed without irreversible chain transfer or chain termination. Recently, advances in living-radical polymerization techniques have led to a number of methodologies that can also be used to produce surfaces exhibiting spatial and temporal polymer distributions that traditional methods simply cannot duplicate.

Of particular interest to this work is the fabrication of grafted polymer surfaces with easily tunable properties such as graft molecular weight, chain length, or chain density. Specially tailored surfaces exhibiting continuous gradients in one or several of these properties represent novel and highly informative tools for both material science and combinatorial chemistry,[3] as they allow for the systematic investigation of surface polymerization kinetics, thermodynamics of surface-tethered macromolecules, copolymer formation including responsive amphiphilic systems, and cell−biomaterial interactions. While a few polymerization[3−9] and microfluidic[10] techniques are available for producing macromolecular gradients either on a surface or within a cross-linked network, the system complexity, time required, cost, and patterning and substrate limitations represent significant drawbacks for their widespread use. For example, Genzer et al. recently used atom-transfer radical polymerization (ATRP), a common living-radical polymerization technique, to create polymer brush surfaces exhibiting gradients in graft density and polymer molecular weight.[3−7] To create the chain density gradients, 1-trichlorosilyl-2-(*m*/*p*-chloromethylphenyl)ethane, the ATRP initiator, was vapor-deposited onto a silicon wafer. The unreacted −OH functionalities were backfilled with *n*-octyltrichlorosilane, an inert, noninitiating compound. After vapor deposition, the films were reacted homogeneously to produce graft density gradient surfaces.[5]

To create the molecular weight gradients, Genzer et al.[3,4] utilized a custom-designed apparatus and a micropump system to control both the slope and thickness of the substrate-bound polymer brush. Graft thicknesses of up to 36 nm were obtained after a 6 h reaction. The slope of the resulting gradient layer was controlled by either manipulating the total reaction time or choosing appropriate ratios of activator and deactivator compounds in the reaction solution.

While ATRP is a robust controlled-radical polymerization method and has been used to pattern substrates with grafted polymer layers,[11−20] its use in creating surfaces exhibiting complex spatial distributions such as gradients, especially those formed on polymeric substrates, is limited. Typically, surface-initiated ATRP involves deposition of thiol- or silane-terminated initiators on either silicon or gold substrates. There are very few cases of ATRP initiators modified to react with, or polymerize from, polymeric base substrates[21] such as cross-linked poly(ethylene glycol). Furthermore, since graft-layer thickness obtained using ATRP is generally controlled via polymerization temperature and time in contact with the polymerization solution containing activator/deactivator complexes, the patterning of complex spatial patterns such as radial gradients, surface-tethered grafts exhibiting multiple minima and maxima in graft length, and even simple striped patterns are difficult to achieve via the polymerization step itself and generally require prior patterning of the underlying initiator layer. These additional steps add complexity, limit substrate

[†] Department of Chemical and Biomolecular Engineering.
[‡] Department of Bioengineering.
* To whom correspondence should be addressed. E-mail: metters@clemson.edu.

10.1021/ma0512051 CCC: $33.50
Published on Web 03/21/2006

compatibility, and make ATRP-based micropatterning very time-consuming.

To overcome the problems presented by ATRP, microfluidics, and other similar techniques in patterning surfaces with well-defined interfacial layers, the current work describes a photopolymerization technique based on the photoiniferter chemistry first discovered by Otsu et al.[22] to produce surface-tethered polymer brush gradients of poly(methyl methacrylate). By using this photoiniferter-mediated photopolymerization (PMPP), we can readily achieve spatial and temporal control over the surface-tethered polymerization by simply controlling the location, intensity, and duration of light exposure across the substrate. Hence, compared to other controlled free-radical polymerization techniques, PMPP is generally faster, can be performed at room temperature with or without solvent, requires no catalyst, is compatible with both organic and inorganic substrates, and can be used to polymerize a wide range of monomers. Furthermore, PMPP not only provides the same lateral micropatterning resolution achievable with traditional photolithographic techniques but also provides nanometer scale resolution in chain length and film thickness.

Photoiniferters are typically dithiocarbamate derivatives capable of initiating multiple radical polymerizations while in the presence of ultraviolet (UV) light. Upon UV photolysis, the photoiniferter undergoes a homolytic bond cleavage yielding a carbon radical and a dithiocarbamyl radical. The carbon-centered radical can react with vinyl monomers while the dithiocarbamyl radical is relatively stable and reacts weakly or not at all with vinyl monomers.[23,24] The dithiocarbamyl radical instead reversibly terminates the growing chain by reacting with the propagating free radicals.[23] This reversible "capping" allows dithiocarbamate derivatives to be used as controlled free-radical initiators in a manner similar to the activator/deactivator complexes necessary in ATRP.

By tethering the photoiniferter to a solid surface, the living nature of photoiniferter-initiated polymerization under the proper reaction conditions should permit precise control over both grafted polymer density and thickness at a given location on a substrate. Since photoiniferters initiate free-radical polymerization when exposed to UV light, complex patterns of surface-tethered polymer layers can theoretically be produced using PMPP by controlling UV wavelength, intensity, or exposure time across the surface. However, the kinetics of PMPPs initiated from substrate surfaces have not been well characterized. Because the dependence of polymerization rate on the previously mentioned reaction conditions is expected to differ from that seen in the bulk, the creation of surfaces exhibiting precise spatially defined properties such as a linear increase in polymer layer thickness with position is not necessarily trivial.[25]

The variation in apparent kinetic behavior for PMPPs presented in the current body of literature is very large. For example, grafted polymer layers ranging in thickness from 150 nm to 1.5 μm have been achieved in reaction times of less than 20 min from photoiniferter-modified polymer substrates.[1,26] Similar photografting experiments performed on photoiniferter-modified silicon substrates indicate variations in grafted film thickness ranging from 150 nm at 3 h exposure time[27] to 60 nm at 20 h irradiation time.[20] Because of these large variations, it is important to develop a systematic and comprehensive method to study the kinetic behavior of photoiniferter-mediated polymerization systems. In addition, the ability to accurately identify the reaction conditions required to achieve a specified graft topography, thickness, or architecture is vital to the design of new nanoscopically modified devices and surfaces.

The ability to pattern surfaces using surface-initiated PMPP techniques has been previously demonstrated by Matsuda and colleaques.[1,26,28] This research included the photolithographic patterning of both poly(ethylene terephthalate) and poly(styrene) substrates derivatized with the photoiniferter benzyl *N*,*N*-diethyldithiocarbamate. Gradient polymer surfaces of continuously increasing thickness were created using either a movable masking system or a gradient neutral-density filter that varied the intensity of transmitted light continuously across the substrate. This work focused primarily on observing the thickness-dependent cellular responses to the fabricated gradient polymer layers. The growth in the thickness of the gradient polymer layers over relatively short exposure times (e.g., less than 30 min) was also measured using atomic force microscopy. However, a comprehensive set of guidelines relating the kinetics and living-polymerization behavior of surface-initiated PMPPs to the rational fabrication of surface-tethered polymer brush gradients was not developed. Such guidelines are vital for future engineering of precisely tailored surfaces with predetermined graft-chain topography, length, density, and molecular weight.

In the current work the kinetic behavior of surface-initiated PMPPs is investigated via gradient polymer brush formation from self-assembled monolayers (SAMs) of photoiniferter. Gradient exposure techniques permit rapid investigation of a broad parameter space while simultaneously minimizing sample-to-sample variations that occur between homogeneous exposures. By using silicon instead of a cross-linked polymer as the substrate, variable angle ellipsometry, a robust surface characterization technique, can be utilized to gain valuable quantitative kinetic information absent from previous gradient studies. The developed fabrication methodology utilizes the architectural and chemical control provided by PMPPs to covalently grow polymer chains of defined lengths and densities from a substrate. It is of specific interest to use the kinetic information derived from ellipsometric measurements to define a set of reaction conditions leading to the formation of surface-tethered macromolecular assemblies whose thickness varies linearly along a flat solid substrate in a predetermined fashion.

A significant advantage of the described gradient PMPP technique is that it allows for high-throughput analysis of surface-tethered polymerization kinetics and polymer chain thermodynamics.[25] The creation of surface-bound graft thickness gradients provides a wealth of data relating important photopolymerization parameters such as exposure time, light intensity, and monomer concentration to polymer molecular weight and grafting density with a fraction of the resources that would be required if only homogeneous exposures were employed. Along with fundamental characterization studies, the gradient technique also opens the door for nanoscale modification of biomaterial surfaces as well as high-throughput analysis of cell−biomaterial interactions by providing a platform to systematically vary cell- or protein-adhesive properties across a biomaterial substrate.

Experimental Section

Materials. The photoiniferter *N*,*N*-(diethylamino)dithiocarbamoylbenzyl(trimethoxy)silane (SBDC) was synthesized and purified as described previously.[20] Sodium diethyldithiocarbamate (Fluka, 97%) was recrystallized from methanol (Fisher Scientific, 99.9%). Prior to use, methyl methacrylate (MMA; Aldrich, 99%) was dehibited by passing over a column of activated, neutral alumina (Sigma). Anhydrous toluene (Alfa Aesar, 99.8%), tetrahydrofuran (Acros, 99.9%), *p*-chlorotrimethoxysilane (Gelest Inc., 95%), sulfuric acid (EMD Chemicals Inc., 95−98%), and hydrogen peroxide (Sigma; 30% v/v in water) were used as received.

Formation of Photoiniferter Self-Assembled Monolayers (SAMs). SBDC SAMs were deposited onto cleaned 1 cm × 1.2

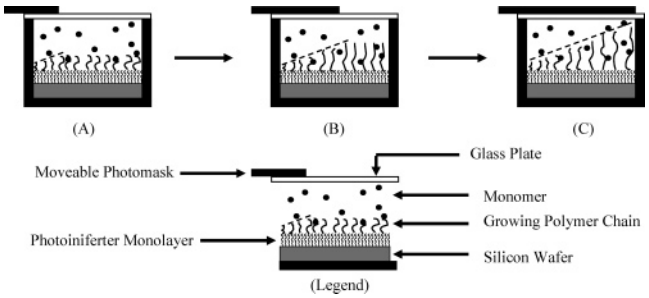

Figure 1. Schematic of gradient polymer growth using the moveable masking system. (A), (B), and (C) show the progression of gradient polymer layer growth as the sample moves under the photomask.

cm silicon wafers as described previously by Rahane et al.[27] Briefly, the silicon wafers were first treated with a strong acidic oxidizing solution of concentrated sulfuric acid and hydrogen peroxide (H_2SO_4:H_2O_2 (30%); 3:1) for ~1 h to introduce reactive hydroxyl functionalities on the silicon surface. After treatment, the wafers were washed with copious amounts of deionized water, dried under a stream of nitrogen, and placed individually in dry test tubes. Each test tube containing a silicon wafer was then flame-dried prior to the addition of a 2 mM solution of SBDC in anhydrous toluene. SAM formation was allowed to proceed for ~16 h, after which the SBDC-SAM surfaces were rinsed and sonicated in pure toluene, dried under nitrogen, and stored in clean, dry test tubes until photopolymerization.

Gradient Photopolymerization. All photopolymerizations were conducted in an oxygen-free environment using a custom-made Teflon reaction cell that has been previously described.[27] The monomer MMA was first dehibited by passage through a column of activated, neutral alumina at room temperature. After dehibition, 5 mL solutions of MMA in anhydrous toluene of concentration 2.34, 3.09, and 4.68 M (corresponding to 25, 33, and 50% v/v, respectively) were prepared in Schlenk flasks and degassed by 4−5 freeze−pump−thaw cycles. In a glovebox, where oxygen levels were maintained at less than 1 ppm, two silicon wafers were placed side-by-side in the reaction cell and covered with monomer solution and a soda lime glass plate.

After assembly, the sealed reaction cell was removed from the glovebox and placed in a custom-designed masking apparatus prior to exposure. The masking system, shown schematically in Figure 1, uses a solid mask and a micropump to create a UV exposure-time gradient across the sample surface. After setting the one-dimensional mask velocity, the assembled reaction cell was exposed to collimated 365 nm light (EXFO 100W Acticure ultraviolet/visible spot-curing system with 365 nm optical filter) at an intensity of 10 mW/cm^2 (measured using an OAI 306 UV powermeter).

The PMMA-modified silicon wafers were sonicated in toluene for 2 h following photopolymerization. Previous results indicate this method is sufficient to remove any bulk polymer entangled within the grafted layer.[27]

Surface Characterization. Static water contact angle and ellipsometric dry layer thickness measurements were used to verify formation of SBDC-SAM surfaces and growth of PMMA grafted layers. For static water contact angle measurements, a Kruss DSA-10 static water goniometer was used with a minimum of three measurements per sample at room temperature. Dry layer thickness measurements were obtained using a Beaglehole Instruments phase modulated picometer ellipsometer with a single wavelength laser probe (He−Ne; $\lambda = 632.8$ nm) across multiple angles of incidence (80−35°) as previously described.[27] Refractive indices of 1.45 and 1.48 were taken for SBDC-SAMs and PMMA grafted layers, respectively.[27] A minimum of three ellipsometric measurements were taken for SBDC-SAM surfaces, while for PMMA gradient films measurements were taken at 0.5 mm intervals across each sample.

The composition and relative density of specific chemical groups across grafted PMMA films were measured using transmission-Fourier transform infrared microscopy (transmission-FTIR). The transmission-FTIR experiments were performed using a Thermo Nicolet Magna 550 FTIR spectrometer equipped with a Nic-Plan FTIR microscope and liquid nitrogen cooled MCT-A detector. The bench and microscope were purged with dry N_2. A total of 32 scans were collected for the sample and background single-beam spectra at a resolution of 4 cm^{-1}. For each gradient sample, transmission-FTIR measurements were taken at 0.5 mm intervals across each film.

Solvent-swollen thicknesses of PMMA films were determined using methods previously described by Samadi et al.[29] Briefly, PMMA gradient films were placed in a custom-designed glass chamber and allowed to swell in the presence of tetrahydrofuran (THF, RI = 1.407), a good solvent for PMMA, for ~15 min prior to analysis. The swollen layer thickness (h_s) was then measured in situ using variable angle ellipsometry (Beaglehole Instruments). Measurements were taken at 1 mm intervals across each film. During the thickness measurements, the refractive index of the swollen PMMA layer was allowed to differ from that of the dry state.

AFM was used to obtain information on the roughness of the grafted polymer surfaces. These data were obtained with a Digital Instruments Bioscope equipped with a NanoScope IIIa controller in "tapping mode". The height (topography) and phase images were captured at 10 μm × 10 μm scan size with a frequency of 1.0 Hz and 256 scans per image. Average surface roughness was determined using the NanoScope Software Version 4.23 root-mean-square (rms) roughness calculation.

Results and Discussion

Characterization of Photoiniferter SAM. The measured ellipsometric thickness of 1.5 ± 0.4 nm for SBDC SAM layers agrees with previously observed SBDC SAM thicknesses.[20,27] On the basis of the measured SAM thickness, the calculated SBDC initiator density present on the surface is ~2.8 molecules/nm^2. This surface-tethered initiator density is consistent with literature SAM surface densities reported for controlled polymerizations.[30] The static water contact angle of the SAM layer was measured at 65 ± 3.2°, consistent with previously obtained values for SAMs of SBDC.[27]

Growth of Gradient Poly(methyl methacrylate) (PMMA) Layers. As surface-confined photoiniferters are exposed to ultraviolet light in the presence of MMA, PMMA chains polymerize from the surface by the so-called "grafting from" approach.[27] The idealized mechanism of PMPP grafting is shown in Scheme 1. Once the individual chains reach a critical size a polymer brush of PMMA is formed on the surface. To create surfaces with gradual variations in polymer molecular weight or grafted chain density, the growth of the polymer brush layer must be precisely controlled with respect to position across the substrate. The rate of surface-initiated photopolymerizations is proportional to the concentration of monomer at the surface [M] and the concentration of surface-tethered, active free radicals [SM$^\bullet$]:

$$R_p = k_p[SM^\bullet][M] \quad (1)$$

where R_p is the rate of polymerization and k_p is the propagation rate constant.[27,31] Every propagation step adds a single monomer unit to the surface-tethered polymer layer. Therefore, the rate of photopolymerization (R_p) is proportional to the rate of increase in the mass of the growing surface-tethered polymer layer ($d\omega/dt$). The thickness of the grafted polymer layer in its dry state (h_d) is related to the mass of the grafted polymer layer (ω) as given in eq 2[21]

$$h_d = \frac{\omega}{A\rho_b} \quad (2)$$

Scheme 1. Idealized Mechanism of Poly(methyl methacrylate) (PMMA) Grafting via Photoiniferter-Mediated Photopolymerization (PMPP)[a]

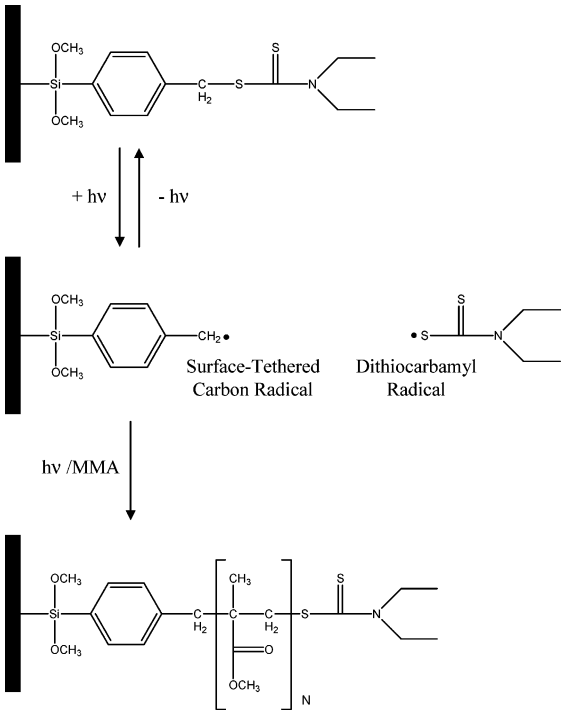

[a] In the presence of ultraviolet light, the surface-tethered photoiniferter undergoes a homolytic bond cleavage yielding a reactive carbon radical and a stable dithiocarbamyl radical. The carbon reactive radical initiates polymerization of MMA monomer to form linear, surface-tethered PMMA while the dithiocarbamyl radical reversibly terminates the growing polymer chain.

where A is the reactive surface area and ρ_b is the bulk polymer density. Equation 2 assumes that the dry polymer layers collapse to their bulk density.[21] Using this information, eq 1 can be rewritten as

$$\frac{dh_d}{dt} = k[SM^\bullet][M] \tag{3}$$

where $k = k_p m_0 V/A\rho_b$, t is the surface UV exposure time, m_0 is the monomer molecular weight, and V is the volume of the bulk monomer solution.

Equation 3 can be extended to further account for the change in dry layer polymer thickness with position on the substrate. This is especially useful for systems employing a movable masking system, where the mask moves at constant velocity across the polymerization cell during the exposure period. The position, x, on the substrate is related to the mask velocity, v, by eq 4.

$$v = \frac{dx}{dt} \tag{4}$$

Therefore, eq 3 can be transformed as follows:

$$\frac{dh_d}{dt}\left(\frac{dt}{dx}\right) = k[SM^\bullet][M]\left(\frac{dt}{dx}\right) = k[SM^\bullet][M]\left(\frac{1}{v}\right) \tag{5}$$

which can be reduced to give eq 6.

$$\frac{dh_d}{dx} = \frac{k}{v}[SM^\bullet][M] \tag{6}$$

Thus, eq 6 indicates that the slope of the dry polymer brush thickness gradient (dh_d/dx) is directly proportional to the surface monomer concentration [M], the concentration of surface-attached, active free radicals [SM$^\bullet$], and the inverse of the mask velocity (v^{-1}).

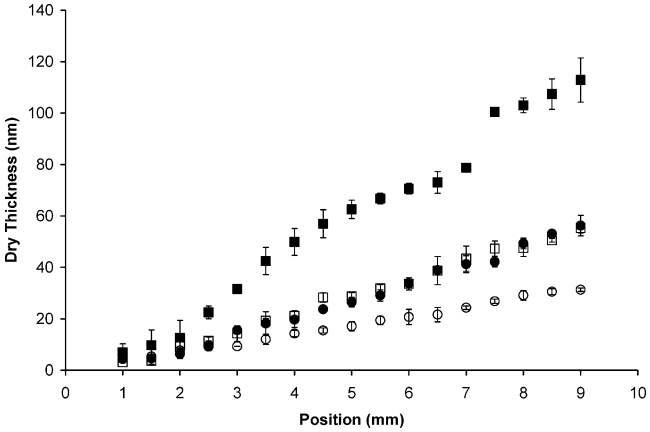

Figure 2. Effect of exposure time and bulk monomer concentration on surface gradient formation: PMMA thickness as a function of position on the silicon substrate. (■) [MMA] = 4.68 M, mask velocity = 6 mm/h, slope = 14 nm/mm; (□) [MMA] = 4.68 M, mask velocity = 12 mm/h, slope = 6.6 nm/mm; (●) [MMA] = 2.34 M, mask velocity = 6 mm/h, slope = 6.7 nm/mm; (○) [MMA] = 2.34 M, mask velocity = 12 mm/h, slope = 3.5 nm/mm. In all cases, UV light intensity (I) = 10 mW/cm^2. Note: values for the slope are taken from linear fits to the data (see Table 1). Error bars represent the range of data for two samples polymerized identically.

Using the quantitative relationships provided above, systematic variation in specific reaction conditions can be used to readily control the slope or steepness of surface-grafted polymer gradients. Examining eq 3, the slope of a polymer layer thickness gradient can be controlled by changing the monomer concentration. Also, from eq 6, the steepness of the thickness gradient with respect to position can be controlled for the reaction system illustrated in Figure 1 by adjusting the mask velocity (e.g., changing surface irradiation time). These features therefore provide two facile methods for tailoring the slope of surface-tethered polymer gradients.

In addition, monomer conversion is low for surface-initiated polymerizations because there is a very low concentration of initiator molecules present on the surface to initiate polymerization (~1−10 molecules/nm^2 substrate). Hence, in the presence of a sufficient amount of bulk monomer, the surface monomer concentration can be assumed to be approximately constant during the course of polymerization.[27,30] Therefore, according to eqs 3 and 6, a constant mask velocity combined with a constant surface-tethered active radical concentration should produce a linear increase in polymer layer thickness with exposure time or position. The linear character of the gradient PMMA layers in Figure 2 indicates constant surface-tethered radical concentrations are maintained during surface-initiated polymerization of MMA up to exposure times of 90 min and layer thicknesses of 120 nm.

Figure 2 also shows the effect of mask velocity and bulk monomer concentration on the PMMA dry layer thickness profile. Samples were exposed in the presence of 4.68 and 2.34 M MMA in toluene using two different mask velocities: 12 and 6.0 mm/h. In all cases the data show a linear increase in dry layer thickness with position. The influence of the mask velocity and monomer concentration on the slope of the surface-bound gradients in Figure 2 is summarized in Table 1. As can be seen, the slopes of the 12 mm/h exposures are approximately half those of the 6 mm/h exposures at the same monomer

Table 1. Dependence of the Slope of Poly(methyl methacrylate) (PMAA) Gradients on Mask Velocity and Monomer Concentration[a]

	mask velocity: 12 mm/h	mask velocity: 6.0 mm/h
[MMA] = 4.68 M	6.6 ± 0.29 nm/mm R^2 = 0.994	14. ± 0.91 nm/mm R^2 = 0.986
[MMA] = 2.34 M	3.5 ± 0.14 nm/mm R^2 = 0.994	6.7 ± 0.35 nm/mm R^2 = 0.991

[a] Slopes are calculated from linear fits to the data presented in Figure 2. R^2 values derived from least-squares fit indicate the high degree of linearity in the data sets.

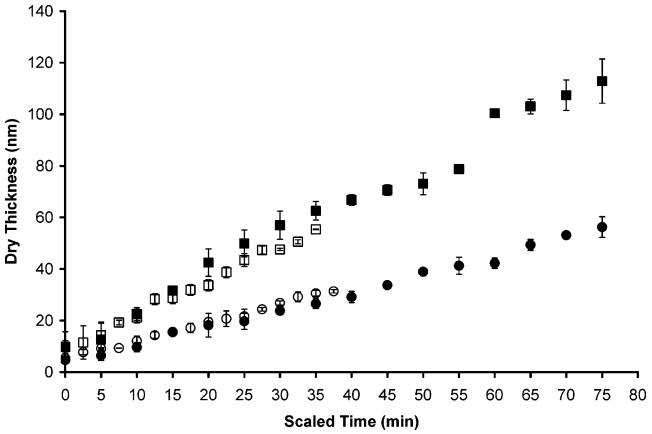

Figure 3. Effect of exposure time and bulk monomer concentration on surface gradient formation: PMMA thickness as a function of exposure time on the silicon substrate. (■) [MMA] = 4.68 M, mask velocity = 6 mm/h; (□) [MMA] = 4.68 M, mask velocity = 12 mm/h; (●) [MMA] = 2.34 M, mask velocity = 6 mm/h; (○) [MMA] = 2.34 M, mask velocity = 12 mm/h. In all cases, I = 10 mW/cm^2. Error bars represent the range of data for two samples polymerized identically.

concentration (48% ratio at 4.68 M; 52% ratio at 2.34 M). Similarly, at a constant mask velocity, the slopes of the 2.34 M exposures are approximately half those of the 4.68 M exposures (53% ratio at 12 mm/h; 49% ratio at 6 mm/h). These results are expected for systems exhibiting constant surface-tethered radical concentrations and confirm a first-order dependence of PMMA layer growth rate on monomer concentration.

While the mask velocity affects the slope of the PMMA thickness gradient with respect to position, it should not change the dependence of brush layer thickness on exposure time. This behavior is confirmed by replotting the thickness data in Figure 2 with respect to exposure time in Figure 3. As shown in the new figure, the previous data sets for a given mask velocity collapse on top of one another and indicate that the slope of the thickness vs exposure time curve is independent of mask velocity. However, as MMA concentration is reduced from 4.68 to 2.34 M, the slope of the resulting curve is reduced by approximately half as predicted by eq 3.

To further validate surface-gradient formation, transmission-FTIR microscopy was used to confirm the presence of the PMMA layer and measure the areal density of surface-tethered MMA carbonyl groups at different positions across the surface. Figure 4a shows the infrared spectra for surface-tethered PMMA at different positions along the gradient surface (4.68 M, 6 mm/h exposure). IR abosrbances corresponding to the carbonyl stretch (C═O), asymmetric stretch (C−CH_3), and C−CH_3 deformation modes of PMMA appear at 1730, 2990, and 1490 cm^{-1}, respectively. A closer look at the C═O stretching region of the transmission-FTIR spectra for gradient PMMA surfaces is shown in Figure 4b. In this figure, the intensity of the carbonyl peak increases across the surface, further indicating the presence of a surface-tethered gradient.

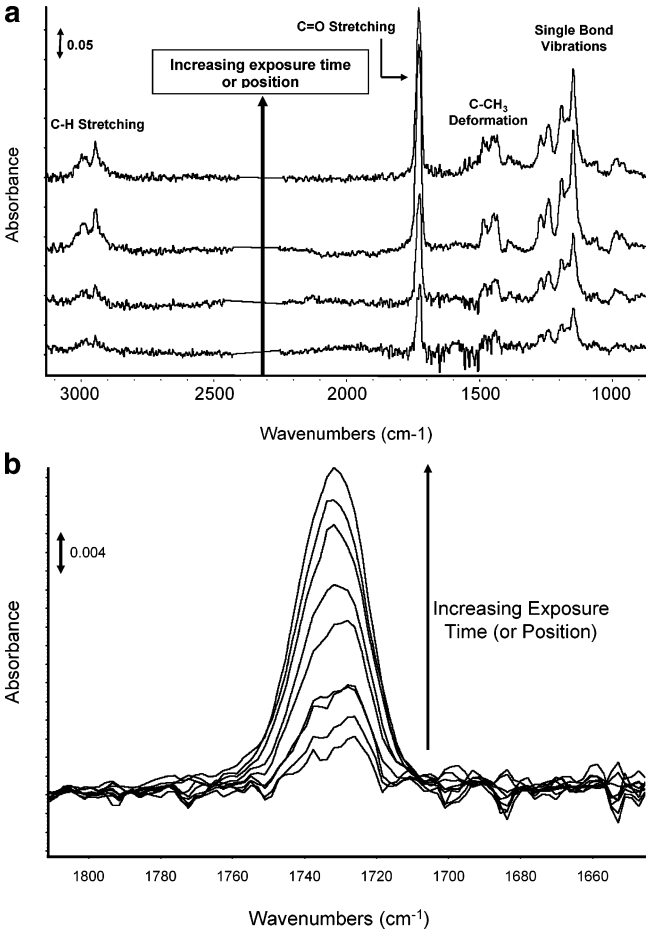

Figure 4. (a) Transmission-FTIR spectra for surface-tethered PMMA taken along the surface gradient. **(b)** Transmission-FTIR spectra of the carbonyl stretching region of PMMA taken at 1 mm intervals along the surface gradient. Exposure conditions: [MMA] = 4.68 M; I = 10 mW/cm^2; mask velocity = 6 mm/h.

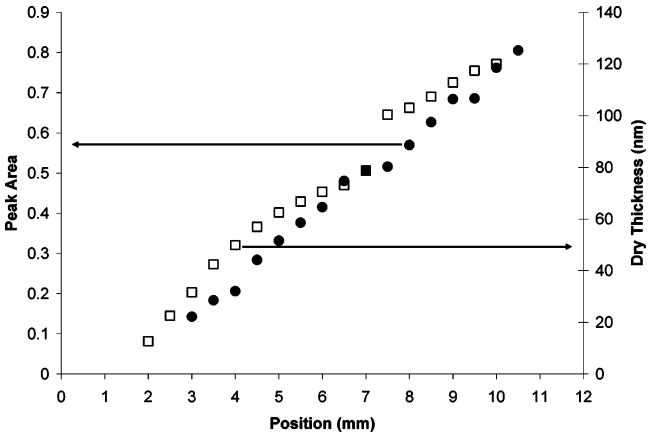

Figure 5. IR peak area of carbonyl stretching region (●) and total PMMA layer thickness (□) as functions of position across the surface. Exposure conditions: [MMA] = 4.68 M; I = 10 mW/cm^2; mask velocity = 6 mm/h.

Figure 5 shows a plot of carbonyl peak area from the FTIR spectra vs position for the C═O stretching region depicted in Figure 4b. The thickness data for this sample are also included (previously presented in Figure 2). The collinear increase in C═O peak area and layer thickness further validate PMMA gradient formation.

To assess how closely the PMMA layer thickness of gradient-polymerized samples match results obtained from homogeneous exposures, four samples were homogeneously irradiated with

Table 2. Summary of in Situ Ellipsometric Swelling Results and RMS Roughness Data Obtained from Atomic Force Microscopy[a]

t (min)	[MMA]	N	M_n (kDa)	R_g (nm)	σ (chains/nm^2)	D (nm)	rms roughness (nm)
25	3.09	3400	341	21.8	0.033	6.2	
35	3.09	3350	336	21.6	0.056	4.8	
45	3.09	3720	373	23.0	0.062	4.5	
30	4.68	6130	614	30.9	0.036	5.9	1.9 ± 0.75
40	4.68	6270	617	31.3	0.056	4.8	
50	4.68	5920	593	30.3	0.074	4.1	6.1 ± 1.1
60	4.68	6160	617	31.0	0.081	4.0	
70	4.68	6310	631	31.4	0.087	3.8	
80	4.68	5940	595	30.4	0.122	3.2	
90	4.68	6090	610	30.8	0.130	3.1	8.6 ± 1.2

[a] Abbreviations: t = exposure time; [MMA] = molar monomer concentration; N = number-average degree of polymerization (eq 7); M_n = number-average molecular weight ($M_n = m_{MMA}N$, where m_{MMA} is the molecular weight of methyl methacrylate); R_g = calculated radius of gyration (eq 10); σ = polymer grafting density (eq 9); D = average distance between polymer chains (eq 11).

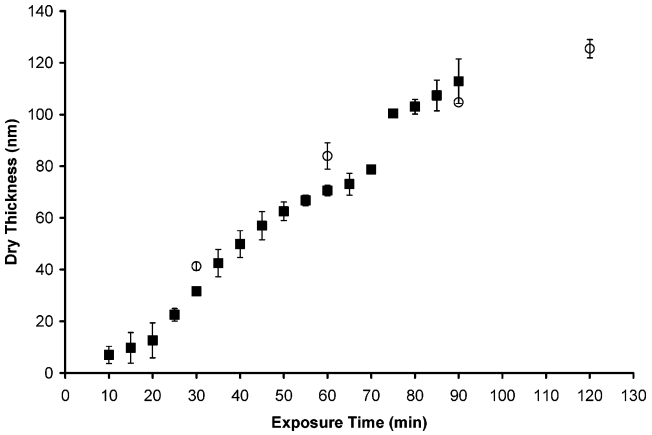

Figure 6. Comparison of gradient exposures (■) and homogeneous exposures (○). For both cases, [MMA] = 4.68 M and I = 10 mW/cm^2. For gradient samples, error bars represent the range of data for two samples polymerized identically. For homogeneous samples, error bars represent 95% confidence intervals; $n = 3$.

UV light for up to 2 h. For the homogeneous samples, the entire sample was exposed for the indicated time. Light intensity (10 mW/cm^2) and monomer concentration (4.68 M) were identical for all samples examined. Figure 6 shows excellent agreement between the gradient and homogeneously polymerized samples. Thus, with only two samples the gradient exposure technique generates a much larger volume of kinetic data relating graft thickness to light intensity, exposure time, and monomer concentration than achieved with more than twice the number of homogeneous exposures. Thus, when compared to traditional photolithographic masking techniques, gradient surface-initiated photopolymerizations not only allow for the creation of novel materials but also provide a tool for rapidly investigating the mechanisms and kinetics of surface-tethered macromolecular assemblies such as polymer brushes.

Finally, atomic force microscopy was used to assess whether layer roughness of the fabricated surface-tethered polymer gradients changes with PMMA layer thickness. As shown in Table 2, the surface roughness, measured at three different points along the gradient, increases with increasing graft thickness. The increase in surface roughness with UV irradiation time has been seen previously on polymer substrates by Matsuda et al. However, the roughness values for those previous samples were at least an order of magnitude higher than what is achieved in the current study using a photoiniferter SAM on silicon.[26] For our system, the maximum roughness value was 8.6 nm at a PMMA thickness of 120 nm, a value similar to films of comparable thickness produced by ATRP and other controlled polymerizations initiated from silicon surfaces.[32,33]

Photoiniferter-mediated photopolymerizations have been described as "living" or "controlled" free-radical polymerizations.[27,34] The defining characteristic of living free-radical polymerizations is the absence of irreversible termination reactions that decrease the free-radical concentration during polymerization. Thus, for living free-radical polymerizations, the concentration of free radicals remains constant during the course of reaction.[35]

For surface-initiated living-radical polymerizations, a linear increase in polymer chain molecular weight with monomer conversion as well as the ability to reinitiate previously grafted polymer layers is generally provided as evidence of living behavior.[4,20] The polymerization data presented in Figures 2−6 are therefore not sufficient to conclude living-polymerization behavior. In other words, it cannot be assumed that the linear PMMA thickness gradients created in this study represent gradients in PMMA molecular weight. The linear nature of the polymer thickness gradient in the dry state may result from variations in grafting density, polymer molecular weight, or a combination of these two factors. Therefore, to investigate both the living character of the polymerization technique and the nature of the gradient layer produced, experiments were conducted to assess polymer grafting density, degree of polymerization, and molecular weight changes across the gradient surfaces.

The ability to directly measure polymer molecular weight and grafting density across a small, flat substrate is not trivial, especially for heterogeneous surfaces. One of the most common methods for determining grafted polymer molecular weight is gel permeation chromatography (GPC). However, in a typical GPC experiment, microgram to milligram quantities of polymer are required for analysis. The low surface areas of the flat silicon substrates used in the current study make it impractical to accumulate a sufficient quantity of uniformly grafted polymer for GPC analysis. Furthermore, GPC analysis requires degrafting of the grafted polymer chains using specially designed degradable initiators and/or harsh chemicals. These methods could dramatically alter the polymerization behavior and final molecular weights of the grafted chains, leading to results that do not accurately reflect the system presented herein.

Another common method of estimating surface-bound polymer molecular weights involves the use of so-called "sacrificial initiators".[14] In this case, a non-surface-confined initiator, similar to that present on the surface, is added to the bulk reaction solution prior to polymerization and is allowed to polymerize concurrently with the surface-bound initiator. Upon completion of polymerization, the obtained bulk polymer can be readily analyzed using GPC to obtain an estimate of the surface-bound polymer molecular weight. However, in the case of the gradient system presented above, a sacrificial initiator presents a significant problem. The introduction of sacrificial initiator into the bulk reaction solution changes the bulk and surface

concentrations of deactivator species. Even slight changes in this concentration have been shown to dramatically affect the polymerization rate and living behavior of surface-initiated, controlled-radical systems and potentially influence the molecular weight of grafted polymer chains.[14]

Therefore, in light of the potential difficulties in applying GPC or sacrificial initiator methods to the current system, the alternative approach of making in situ ellipsometric swelling measurements across the gradient surfaces was implemented to estimate changes in polymer molecular weight and grafting density (σ) with exposure time. These characteristic parameters can be estimated from the measured swollen and dry layer thicknesses of a polymer brush based on calculations first described by Milner[36] and later implemented by Jordan et al.[37] and Samadi et al.[29] According to these previous investigations, the number-average degree of polymerization (N) of polystyrene (PS) brushes swollen in toluene can be estimated from eq 7:[29,36,37]

$$N = [1.074(h_s)^{3/2}]/[(h_d)^{1/2}] \tag{7}$$

where h_s and h_d are swollen and dry layer ellipsometric thicknesses, respectively.

To determine whether eq 7 is also a valid model for predicting the swelling behavior of PMMA in THF, the properties of both PS and PMMA and their interactions with each respective solvent were compared. The characteristic ratio (C_∞), a measure of chain stiffness, is 10.8 and 7.0 for PS and PMMA, respectively,[38,39] while the skeletal bond length (l) is essentially identical for PS and PMMA (0.153 nm).[40] The solvent quality of both polymer−solvent systems was estimated from values of the Flory−Huggins interaction parameter (χ) found in the literature.[41] For polymer molecular weights of $\sim 10^5$ g/mol, χ for PS in toluene at 27° C ($\chi_{PS,TOL}$) is 0.455, while $\chi_{PMMA,THF}$ at 27° C is 0.459.[41] Thus, the interaction of PMMA and PS with their respective good solvent and the excluded volume of each polymer chain will be approximately the same.[42]

To further confirm the validity of using eq 7 to characterize our PMMA brushes, the linear expansion coefficient (α) of PMMA in THF ($\alpha_{PMMA,THF}$) and PS in toluene ($\alpha_{PS,TOL}$) were directly compared using eq 8 and the parameter values given above.[42]

$$\alpha \approx \left(\frac{C_\infty}{6}\right)^{-3/10}(1-2\chi)^{1/5}N^{1/10} \tag{8}$$

The value of N in eq 8 was based on the molecular weight of the polymer at which χ was determined (10^5 g/mol).[41] α is the measure of chain expansion based on polymer−solvent interactions.[42] Application of eq 8 to each polymer−solvent system gives $\alpha_{PMMA,THF} = 1.19$ and $\alpha_{PS,TOL} = 1.22$. The close agreement in these values ($\alpha_{PS,TOL}/\alpha_{PMMA,THF} = 1.02$) indicates the degree of polymer expansion from dry to swollen state should be nearly the same for both systems. Thus, based on the similar polymer dimensions, stiffnesses, excluded volumes, and swelling behavior, eq 7, a model derived for PS in toluene, should also adequately approximate the swelling behavior of PMMA in THF and give a reasonable estimate of N for this system. Furthermore, the approximation of N provided by eq 7 is valid for the purposes of this work, where the goal is to examine trends in grafting density and polymer molecular weight across the surface rather than to provide absolute measurements of N.

Once N has been determined with respect to position across the substrate, changes in grafting density (σ) and radius of gyration (R_g) of swollen PMMA chains across the gradient surfaces can be calculated using eq 9[21,29,43] and eq 10,[39] respectively.

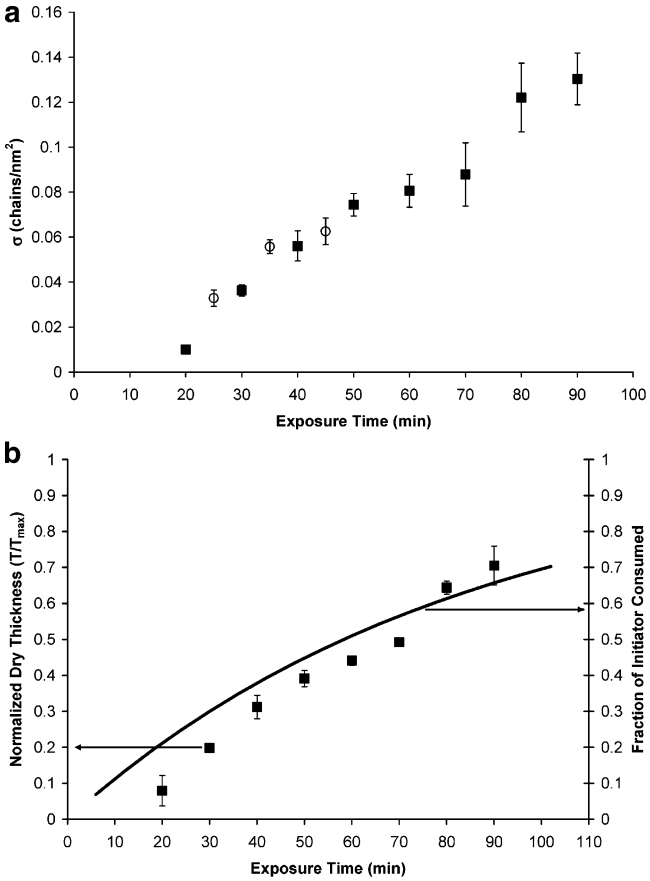

Figure 7. (a) Polymer grafting density as a function of exposure time and monomer concentration. Exposure conditions: (■) [MMA] = 4.68 M; I = 10 mW/cm²; mask velocity = 6 mm/h; (○) [MMA] = 3.09 M; I = 10 mW/cm²; mask velocity = 6 mm/h. (b) Comparison of normalized dry thickness increase in PMMA layers (■) and initiator consumption (solid line) with exposure time. Exposure conditions: [MMA] = 4.68 M; I = 10 mW/cm², mask velocity = 6 mm/h. Model coefficients: I = 10 mW/cm², ϵ = 100 L/(mol cm), f = 0.065.

$$\sigma = \frac{\rho_b h_d N_A}{m_0 N} \tag{9}$$

$$R_g\,(\text{Å}) = 1.71N^{0.596} \tag{10}$$

Note that in eq 9 N_A represents Avogadro's number. When the degree of polymerization (N) and density of grafted PMMA chains (σ) are obtained, the distance between grafting sites (D) can be calculated using eq 11.[29]

$$D = (4/\pi\sigma)^{1/2} \tag{11}$$

Table 2 summarizes the results of swelling experiments across two PMMA thickness gradient surfaces. Since the brush regime is generally characterized by $D < 2R_g$,[29,44] the values in Table 2 confirm formation of dense PMMA brush layers across both representative gradient surfaces. In addition, as shown in both Table 2 and Figure 7a, at constant monomer concentration, the polymer grafting density increases linearly with exposure time across the surface while the number-average degree of polymerization and molecular weight of the grafted chains remain essentially constant. Taken together, these results suggest that the observed gradient in PMMA graft thickness results from a

gradient in grafting density, and not polymer molecular weight or degree of polymerization.

It is also important to note the dependence of grafted polymer molecular weight on bulk monomer concentration during polymerization. As shown in Table 2, when the monomer concentration is reduced by one-third from 4.68 to 3.09 M, the molecular weight of the polymer chains decreases by approximately one-third, indicative of a first-order dependence of polymer molecular weight on monomer concentration. This first-order dependence also explains the controlled doubling of the slope of the PMMA thickness gradient seen in Figures 2 and 3 when monomer concentration is doubled.

The results of Table 2 also provide insight into the living nature of the photoiniferter-mediated polymerization system used to produce the gradient PMMA brush surfaces. Although graft layer thickness is increasing linearly with exposure time (or position), as shown in Figures 2 and 3, swelling results used in Table 2 indicate that the molecular weights of the PMMA chains are constant with exposure time. This characteristic implies nonliving polymerization behavior where the rate of initiation (R_i) is much slower than the rate of propagation (R_p). This result contradicts bulk solution polymerization behavior of photoiniferter systems where R_i is much greater than R_p and the molecular weight of the polymer chains increases with polymerization time.[45]

Initiation kinetics were modeled to lend additional insight into the mechanism of gradient formation. For free-radical photopolymerizations, the rate of initiation is[31]

$$\frac{d[I_n]}{dt} = -k_d[I_n] = -\epsilon f I[I_n] \qquad (12)$$

where k_d is the initiator dissociation constant, I_n is the concentration of initiator, f is the initiator efficiency (0.065), ϵ is the experimentally determined initiator extinction coefficient (100 L/(mol cm)), I is the incident light intensity (10 mW/cm^2), and t is exposure time. The overall initiator efficiency of 6.5% was determined from a ratio of the maximum PMMA grafting density across the gradient surface and the surface initiator density.[46] The rate of initiator consumption will determine the time-dependent increase in the grafting density of the polymer brush. As shown in Figure 7b, dry layer thickness and initiator consumption for a given gradient sample increase concurrently with exposure time. The agreement between these model predictions and experimental data further indicates that the resulting gradient in PMMA layer thickness across the surface is a direct result of a grafting density gradient resulting from nonliving polymerization behavior. It should be noted that in Figure 7b the limiting thickness value used to normalize the dry layer PMMA thickness was 160 nm. This is the maximum thickness obtained for a 2 h homogeneous PMMA photopolymerization under otherwise identical conditions to those used for the gradient exposures. After 2 h, Rahane et al. demonstrated that termination effects dominate, resulting in no further increase in dry layer thickness for 10 mW/cm^2, 4.68 M PMMA exposures.[27] Therefore, 160 nm was taken as the maximum obtainable thickness value (T_{max}) and thus was used to normalize the gradient thickness data presented in Figure 7b.

For the observed surface-initiated polymerization, it is hypothesized that the nonliving behavior arises from the very low concentration of available dithiocarbamate "deactivating" radicals near the growing polymer layer. These deactivating radicals are needed to reduce the overall population of active radicals at any given instant, thus reducing the rate of propagation and unwanted termination reactions. It is believed that these untethered radicals diffuse away from the surface and into the bulk monomer solution soon after initiation, significantly reducing the reversible capping of active surface radicals, accelerating the rates of propagation and termination, and rendering the system uncontrolled.

To assess whether the surface-tethered PMMA chains were undergoing reversible termination via dithiocarbamate capping, a reinitiation experiment was conducted in which previously polymerized PMMA gradient films were exposed to UV light in the presence of a second monomer, styrene, for 2 h. A typical observation of photoiniferter-mediated living polymerization behavior is the ability to reinitiate polymer films and produce a diblock or triblock copolymer.[20,22,34,45,47] For the PMMA gradient films, upon reinitiation for 2 h, no appreciable change in the graft thickness was seen (data not shown). The absence of reinitiation has also been confirmed on homogeneously polymerized SBDC silicon substrates where no additional deactivating radicals were added prior to initial exposure.[48]

The reinitiation results of this study conflict with previous findings from de Boer et al. and Otsu et al., both of whom were able to create diblock (or triblock) copolymers upon reinitiation of surface-grafted layers fabricated using photoiniferter-mediated polymerizations.[20,47] Otsu et al. demonstrated that molecular weight and grafting yield of homogeneous polymers grown from photoiniferter-modified silica beads increased with UV exposure time, indicating that the surface graft copolymerization proceeded in a manner similar to the living-like radical mechanism observed in solution. In addition, they also provided evidence that the block chain lengths of diblock and triblock copolymers grafted on the surfaces were precisely controlled.[47] However, their results, obtained from surface-initiated polymerizations on silica beads, do not necessarily apply to flat silicon substrates such as those used in this study where surface areas, initiator densities, and dithiocarbamate radical densities are significantly lower than those present on silica beads. Furthermore, it is difficult to directly compare a curved silica surface to the flat SAM surfaces used in the current study since they sterically present an entirely different system that could affect the initiation and propagation kinetics as well as the conformation of the growing polymer brush.[37]

In the case of de Boer et al., the reported polymer growth rates were much lower than those observed in the current system even though the same photoinitiating SAM layer was used.[20] The dramatically lower growth rates indicate that additional deactivating species could have been added to improve the living characteristics of their system. However, it is impossible to give a more direct comparison to the current study since the specific reaction conditions used by de Boer et al. were not provided.

Conclusions

The results of the swelling studies presented above, along with the ellipsometric and infrared analyses, provide an overall picture of polymer grafting via gradient, photoiniferter-mediated polymerizations. Under the conditions studied, the linearity of PMMA graft layer thickness with respect to exposure time (or position) (Figures 2 and 3) arises due to a gradient in the density of polymer chains of constant molecular weight (Table 2 and Figure 7). Further, the polymerization appears to be nonliving as shown by both molecular weight evolution and the results of reinitiation studies.

However, because the polymerization is nonliving does not mean it is uncontrolled. The methodology presented above allows linear polymer gradients up to 120 nm in thickness to

be patterned on flat substrates over relatively short exposure times (<90 min). Different gradient slopes and absolute thicknesses can be achieved by judiciously varying monomer concentration or photomask velocity. Furthermore, since polymer chain density in the current system is readily determined via UV exposure time, this technique simplifies previous methods for fabricating graft density gradients by eliminating the need for vapor deposition or other initiator patterning techniques prior to polymerization.

Although not investigated in this work, the effects of light intensity and surface initiator density on photoiniferter-mediated grafting are important design variables when creating micropatterned surfaces. It has been shown that variations in light intensity and surface initiator density can significantly impact polymerization rate, the configuration of surface attached polymer layers, and the prevalence of nonliving termination reactions.[27,31] Thus, these additional parameters can substantially impact polymerization behavior and, in the case of this paper, surface gradient formation. Currently, gradient formation using a photomask that varies light intensity linearly across the surface is being investigated. By knowing the kinetics of photoiniferter-mediated brush formation upon variations in light intensity, these systems can be optimized in order to create more precise surface profiles for a variety of monomer systems.

A major advantage of the current work is that it presents a method for rapid analysis of surface photopolymerization kinetics. The MMA polymer layers grown using the gradient exposure technique exhibited linear increases in thickness with exposure time. The rate of thickness increase with time was first order with both monomer concentration and exposure time. Furthermore, the thicknesses achieved using the gradient exposure technique were similar to those obtained via homogeneous exposures, indicating that polymerization behavior is nearly identical between the two polymerization methods. Therefore, the gradient exposure technique provides a means of generating a much larger volume of kinetic data relating graft thickness to light intensity, exposure time, and monomer concentration in fewer samples than would be required with homogeneous exposures. Finally, all polymerizations described in the current work were performed in less than 2 h, much less time than is required to achieve similar graft thicknesses with living polymerization techniques.[3−7,10−20] Thus, this gradient polymerization technique provides a facile method for modifying inorganic and organic substrates with exact densities of polymeric molecules and achieving nanometer-scale resolutions in layer thickness.

Acknowledgment. We gratefully acknowledge the NSF-sponsored Center for Advanced Engineering of Fibers and Films (Award No. EEC-9731680), NSF-EPSCoR, and ORAU (through a Ralph E. Powe Award to A.T.M.) for financial support. We also gratefully acknowledge Kimberly Ivey for FTIR microscopy, Azadeh Samadi for assistance with swelling studies, Santosh B. Rahane for SBDC synthesis and extensive technical support, and Profs. Igor Luzinov and S. Michael Kilbey for helpful discussions.

Note Added after ASAP Publication. This paper was pulled from the Web on January 25, 2006. Revisions were made to the text and Table 2, and the article was reposted on March 21, 2006.

References and Notes

(1) Nakayama, Y.; Matsuda, T. *Macromolecules* **1996**, *29*, 8622−8630.
(2) Wong, J. Y.; Velasco, A.; Rajagopalan, P.; Pham, Q. *Langmuir* **2003**, *19*, 1908−1913.
(3) Tomlinson, M. R.; Genzer, J. *Macromolecules* **2003**, *36*, 3449−3451.
(4) Tomlinson, M. R.; Genzer, J. *Chem. Commun.* **2003**, 1350−1351.
(5) Wu, T.; Efimenko, K.; Vlcek, P.; Subr, V.; Genzer, J. *Macromolecules* **2003**, *36*, 2448−2453.
(6) Efimenko, K.; Genzer, J. *Adv. Mater.* **2001**, *13*, 1560−1563.
(7) Genzer, J.; Fischer, D. A.; Efimenko, K. *Adv. Mater.* **2003**, *15*, 1545−1547.
(8) Desilles, N.; Lecamp, L.; Lebaudy, P.; Bunel, C. *Polymer* **2003**, *44*, 6159−6167.
(9) Desilles, N.; Lecamp, L.; Lebaudy, P.; Bunel, C. *Polymer* **2004**, *45*, 1439−1446.
(10) Burdick, J. A.; Khademhosseini, A.; Langer, R. *Langmuir* **2004**, *20*, 5153−5156.
(11) Husseman, M.; Mecerreyes, D.; Hawker, C. J.; Hedrick, J. L.; Shaw, R.; Abbot, N. L. *Angew. Chem., Int. Ed.* **1999**, *38*, 647−649.
(12) Shah, R.; Mecerreyes, D.; Hussemann, D.; Rees, I.; Abbot, N. L.; Hawker, C. J.; Hedrick, J. L. *Macromolecules* **2000**, *33*, 597−605.
(13) Jeon, N. L.; Choi, I. S.; Whitesides, G. M.; Kim, N. Y.; Laibinis, P. E.; Harada, Y.; Finnie, K. R.; Girolami, G. S.; Nuzzo, R. G. *Appl. Phys. Lett.* **1999**, *75*, 4201−4203.
(14) Matyjaszewski, K.; Miller, P. J.; Shulka, N.; Immaraporn, B.; Gelman, A.; Luokala, B. B.; Siclovan, T. M.; Kickelbick, G.; Vallant, T.; Hoffmann, H.; Pakula, T. *Macromolecules* **1999**, *32*, 8716−8724.
(15) Ghosh, P.; Lackowski, W. M.; Crooks, R. M. *Macromolecules* **2001**, *34*, 1230−1236.
(16) Jones, D. M.; Huck, W. T. S. *Adv. Mater.* **2001**, *13*, 1256−1259.
(17) Jones, D. M.; Brown, A. A.; Huck, W. T. S. *Langmuir* **2002**, *18*, 1265−1269.
(18) Osborne, V. L.; Jones, D. M.; Huck, W. T. S. *Chem. Commun.* **2002,** 1838−1839.
(19) Hyun, J.; Chilkoti, A. *Macromolecules* **2001**, *34*, 5644−5652.
(20) de Boer, B.; Simon, H. K.; Werts, M. P. L.; van der Vegte, E. W.; Hadziiannou, G. *Macromolecules* **2000**, *33*, 349−356.
(21) Liu, Y.; Klep, V.; Zdyrko, B.; Luzinov, I. *Langmuir* **2004**, *20*, 6710−6718.
(22) Otsu, T.; Yoshida, M.; Tazaki, T. *Macromol. Chem. Rapid Commun.* **1982**, *3*, 133−140.
(23) Lambrinos, P.; Tardi, M.; Polton, A.; Sigwalt, P. *Eur. Polym. J.* **1990**, *26*, 1125−1135.
(24) Kazmaier, P. M.; Moffat, K. A.; Georges, M. K.; Veregin, R. P. N.; Hamer, G. K. *Macromolecules* **1995**, *28*, 1841−1846.
(25) Semler, J. J.; Genzer, J. *Macromol. Theor. Simul.* **2004**, *13*, 219−229.
(26) Higashi, J.; Nakayama, Y.; Marchant, R. E.; Matsuda, T. *Langmuir* **1999**, *15*, 2080−2088.
(27) Rahane, S. B.; Kilbey II, S. M.; Metters, A. T. *Macromolecules* **2005**, *38*, 8202−8210.
(28) Nakayama, Y.; Matsuda, T. *Macromolecules* **1999**, *32*, 5405−5410.
(29) Samadi, A.; Husson, S. M.; Liu, Y.; Luzinov, I.; Kilbey, S. M., II *Macromol. Rapid Commun.* **2005**, *26*, 1829−1834.
(30) Gopireddy, D.; Husson, S. M. *Macromolecules* **2002**, *35*, 4218−4221.
(31) Odian, G. In *Principles of Polymerization*, 4th ed.; Wiley-Interscience: New York, 2004; pp 198−350.
(32) Zhao, B.; Brittain, W. J. *Macromolecules* **2000**, *33*, 342−348.
(33) Granville, A. M.; Boyes, S. G.; Akgun, B.; Foster, M. D.; Brittain, W. J. *Macromolecules* **2004**, *37*, 2790−2796.
(34) Otsu, T. *J. Polym. Sci., Part A: Polym. Chem.* **2000**, *38*, 2121−2136.
(35) Huang, X.; Wirth, M. J. *Macromolecules* **1999**, 32, 1694−1696.
(36) Milner, S. T. *Europhys. Lett.* **1988**, *7*, 695−699.
(37) Jordan, R.; Ulman, A.; Kang, J. F.; Rafailovich, M. H.; Sokolov, J. *J. Am. Chem. Soc.* **1999**, *121*, 1016−1022.
(38) Brandrup, J.; Immergut, E. H.; Grulke, E. A. In *Polymer Handbook*, 4th ed.; Wiley-Interscience: New York, 1999; p VII-55.
(39) Jackson, C.; Chen, Y.-J.; Mays, J. W. *J. Appl. Polym. Sci.* **1996**, *61*, 865−874.
(40) Yoon, D. Y.; Flory, P. J. *J. Polym. Sci., Polym. Phys. Ed.* **1976**, *14*, 1425−1431.
(41) Qian, J. W.; Rudin, A. *Eur. Polym. J.* **1992**, *28*, 725−732.
(42) Fleer, G. J.; Cohen Stuart, M. A.; Scheutjens, J. M. H. M.; Cosgrove, T.; Vincent, B. In *Polymers at Interfaces*; Chapman and Hall: London, 1998; pp 1−9.
(43) Luzinov, I.; Tsukruk, V. V. *Macromolecules* **2002**, *35*, 5963−5973.
(44) Kilbey II, S. M.; Watanabe, H.; Tirrell, M. *Macromolecules* **2001**, *34*, 5249−5259.
(45) Otsu, T.; Ogawa, T.; Yamamoto, Y. *Macromolecules* **1986**, *19*, 2089−2091.
(46) Pruker, O.; Ruhe, J. *Macromolecules* **1998**, *31*, 602−613.
(47) Otsu, T.; Matsunaga, T.; Doi, T.; Matsumoto, A. *Eur. Polym. J.* **1995**, *31*, 67−78.
(48) Rahane, S. B.; Kilbey II, S. M.; Metters, A. T. Manuscript in preparation.

MA0512051